ACCSCIENCE PUBLISHING

Green Technology & Innovation

ARTICLE

Minimizing shadow effects to optimize solar energy input in the World Solar Challenge

Pradyum Kaneria* and **K. S. Reddy***

Heat Transfer and Thermal Power Laboratory, Department of Mechanical Engineering Indian Institute of Technology Madras, Chennai, Tamil Nadu, India

Abstract

Efficient energy utilization is essential for the performance of solar-powered electric vehicles, especially for achieving extended range in competitive settings such as the World Solar Challenge (WSC25). This 3,000 km race from Darwin to Adelaide, Australia, presents unique challenges, particularly regarding efficiently capturing solar energy using a 6 m^2 panel area. Factors such as the type of solar cells, their orientation, and the photovoltaic (PV) arrangement in clusters mapped to maximum power point tracking systems play significant roles in energy efficiency. This study examines the shading effects encountered during WSC25 on a vehicle measuring 5.5 m in length, 1.6 m in width, and 1 m in height, with a drag coefficient of 0.0973. We assessed the impact of shading on energy generation and vehicle performance. By analyzing solar irradiance along the race route using Hotell's clear-day model, we aimed to optimize the roof angle of the solar panels to enhance energy absorption. The vehicle was equipped with a 3.35 kWh battery and 1.32 kWh solar panels, rated under standard test conditions. We also identified areas prone to shading that may affect the overall energy yield, utilizing Blender for visualization. A comprehensive energy audit was conducted to quantify power losses associated with shading and other factors influencing vehicle performance. Furthermore, we explored potential strategies to mitigate these losses and improve overall energy input, including the use of bypass diodes in specific shadow-affected regions. Our findings show that the use of half-cut solar cells in shaded regions can enhance energy generation by 3% compared to the best-performing full-cut cell cluster under similar shading conditions. These insights offer valuable guidance for the design of solar vehicles and the development of race strategies for teams competing in solar endurance challenges worldwide.

Keywords: Energy audit; Shadow effect; Solar energy maximization; Solar vehicle; World Solar Challenge

***Corresponding author:**
Pradyum Kaneria (me21b142@smail.iitm.ac.in)
K.S. Reddy (ksreddy@iitm.ac.in)

Citation: Kaneria P, Reddy KS. Minimizing shadow effects to optimize solar energy input in the World Solar Challenge. *Green Technol Innov*. 2025;1(1):025090004. doi: 10.36922/GTI025090004

Received: February 27, 2025

1st revised: April 6, 2025

2nd revised: April 12, 2025

Accepted: April 14, 2025

Published online: May 5, 2025

1. Introduction

The World Solar Challenge (WSC) is a prestigious biennial event held in Australia, attracting teams from around the world to showcase their innovative solar-powered vehicles. With each iteration, new rules and specifications are introduced to push the boundaries of solar vehicle technology and promote sustainable energy solutions. For the upcoming race, the allowable solar panel area per vehicle has been increased to 6 m^2, while the permitted energy storage capacity has been decreased. This significant change

in specifications requires teams to rely more heavily on solar power to propel their vehicles across the grueling 3,000 km race route from Darwin to Adelaide, as illustrated in Figure 1. As a result, both a well-developed solar vehicle design and a meticulously planned race strategy become crucial for successfully finishing the race. To navigate the challenging race conditions, teams employ robust data-driven algorithms to predict their next moves and optimize their energy consumption. An intricate energy model is essential, taking into account various factors such as energy losses and gains, weather conditions (e.g., wind gusts, solar irradiance, and cloud cover), shadow effects on solar panels, traffic conditions, and road gradients.

Energy modeling is also important for managing energy efficiently over gradual inclines during the first half of the race and capitalizing on descents to conserve energy, as shown in Table 1 and Figure 2, which detail the terrain encountered during the WSC. Many solar vehicles in the competition feature an extruded area to accommodate the driver's compartment and provide necessary visibility. However, this design can cast shadows on adjacent solar panels, thereby reducing their effectiveness. Managing such shadow effects is therefore crucial.

To maximize energy capture, solar panels must be tightly packed on the vehicle's roof to utilize the full 6 m^2 allocation without increasing the vehicle's overall length or width, as such increases could lead to aerodynamic losses. To create a highly efficient competition solar vehicle, each design parameter must be effectively optimized, and the impact of shadows on the net energy audit must be thoroughly understood and incorporated into the team's strategy. This approach is essential for making informed decisions and minimizing energy losses, thereby capitalizing on even small amounts of energy harvested each second – which, when accumulated, can make a significant difference over the duration of the race. Therefore, ongoing research aims to accurately predict shadow losses and their impact on total energy production, as well as to propose effective strategies for minimizing these losses and maximizing

Table 1. Coordinates and elevation data along the race route

Place	Latitude	Longitude	Elevation (m)
Darwin	−12.455726	130.837174	28
Katherine	−14.460721	132.257229	106
Dunmarra Highway Inn	−16.763859	133.427909	5952
Elliot	−17.552167	133.543023	220
Tennant Creek	−19.636566	134.192022	366
Barrow Creek	−21.378259	133.976667	511
Alice Spring	−23.707679	133.873851	550
Coober Pedy	−29.023372	134.752121	221
Glendambo	−30.969752	135.748780	150
Port Augusta	−32.501381	137.779848	21
Adelaide	−34.929355	138.586994	66

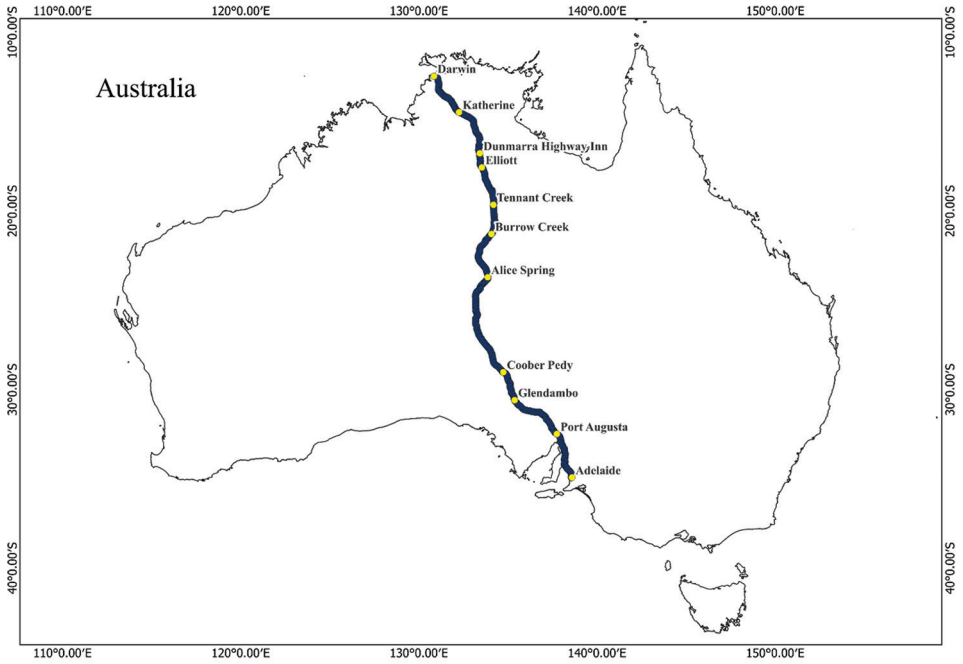

Figure 1. The marked path represents the route from Darwin to Adelaide, Australia, with control stops indicated

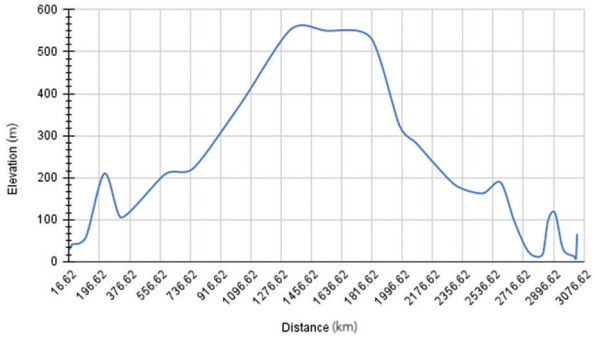

Figure 2. Elevation versus distance profile along the race route

energy efficiency throughout the race. Extensive studies are being conducted on the effects of shadows and potential mitigation methods. Partially shaded solar panels experience reduced power irradiance levels and, in some cases, may even absorb energy instead of generating.[1]

Traditional solutions primarily focus on optimization at the panel level but often overlook the impact of partial shadowing at the sub-string level, which can also compromise efficiency. To address this, researchers have developed compensation circuits to enhance energy input at the sub-string level by redistributing energy. These circuits draw energy from unshaded sub-strings and output compensation currents to regulate the operating point of the shaded sub-strings.[2] The series or parallel connection also plays a crucial role in determining energy loss due to shadow, mainly because the current output of a shadowed cell can limit the performance of the entire cluster.[3] Initial developments to enhance energy input have focused on stationary solar panels. However, extending such technologies to solar vehicles – an emerging and promising alternative in sustainable mobility – presents new challenges due to dynamically changing shadow patterns caused by buildings or road gradients. Considerations and strategic planning are important, and the development of commercial solar vehicles is already underway.[4] One promising area of advancement is onboard charging, which can significantly reduce dependence on grid-based charging systems throughout the year for both private and public transportation.[5] While past research[6] explores multiple vehicle charging methods, including those designed for diverse commuter needs, it does not limit the discussion to grid-based systems. Onboard charging holds substantial potential for extending the driving range and reducing the frequency of charging during long-distance travel.

Other emerging charging methods include traction and wireless systems. Traction charging involves a wired cable embedded along travel routes – similar to tram systems – but faces economic and infrastructural challenges due to the need for dedicated roadways. Wireless charging emerges as a promising alternative, although its high infrastructure costs hinder widespread adoption. While grid-based charging offers extended charging durations and facilitates the establishment of a global infrastructure network, it too has limitations. In contrast, onboard charging emerges as a more sustainable solution.

Previous research[7] includes system modeling of similar solar vehicles but does not account for energy losses due to shadow cast by vehicle structures such as canopies, nor does it consider panel azimuth – both of which are important factors in energy generation. Extending the study of onboard charging and shadow effects to competitive solar vehicles is crucial for developing a more precise strategy model to accurately predict solar energy losses.

Driving an aerodynamic vehicle over 3,000 km through constantly changing weather and terrain conditions poses significant challenges, necessitating meticulous planning and decision-making in advance. Therefore, maximizing solar energy input becomes a paramount objective. Various techniques can be employed to increase energy input from solar panels. One approach involves using a larger panel area, although this comes at the cost of increased surface area. Another option is to incorporate high-efficiency solar cells, such as perovskite tandem cells, which offer efficiencies of 30% or more but are relatively costly. Additional strategies include minimizing partial shadow conditions on the panels and enhancing external factors such as solar irradiance capture. Among these, the most economical and adaptable method is to orient the solar cells to capture the highest possible irradiance. This requires careful consideration of the optimal angle for each section of the roof, as variables such as tilt and curvature can impact both irradiance and aerodynamic performance.

It is crucial to strike a balance between aerodynamic forces – such as drag and lift – and power input to achieve optimal performance. To determine the optimal roof angle across different vehicle sections, an empirical irradiance prediction solar energy input model is used in conjunction with time-of-day and solar position data. Once the optimal orientation is identified, the solar vehicle's body shell is adjusted to minimize the drag coefficient (Cd) while adhering to the regulations set by WSC. Furthermore, solar panels affected by shadows are identified, and various strategies are simulated to maximize their solar energy capture. During this process, the threshold value of the maximum power point tracking (MPPT) system is carefully considered to ensure efficient energy conversion. With these considerations in mind, the solar vehicle's energy input can be optimized while maintaining aerodynamic efficiency. To

reduce aerodynamic drag while ensuring driver visibility, the vehicle incorporates a protruding canopy. However, this feature may cast shadows on surrounding solar panels depending on the Sun's position. Other causes of shadow effects include elevated terrain near the race route. Shading has a significant impact on solar vehicle performance, particularly in long-distance endurance races such as WSC. Even partial shading of photovoltaic (PV) panels can lead to disproportionate losses in power output due to the series configuration of cells, resulting in a voltage drop across the entire array. If the array voltage drops below the MPPT threshold, power generation may cease altogether. The present study examines strategies to enhance energy output, which can guide the design of energy-optimized solar electric vehicles.

2. Modeling of solar vehicle

The present study uses advanced models to address the shadow effect and minimize its impact on solar energy output. One of these is a solar prediction model, which enables accurate forecasting of irradiance levels. By predicting solar radiation, we can optimize the performance and angle of the vehicle's solar panels to maximize energy production during the race. In addition, we implemented an energy audit model that continuously monitors energy usage. This model provides valuable insights into energy consumption patterns, allowing the identification of areas for improvement and the development of strategies to optimize energy utilization. These models were built using empirical relations and demonstrated high accuracy in initial calculations and comparisons.

By utilizing these sophisticated models, we were able to explore various options for enhancing solar energy output in solar vehicles. For visualization purposes, a reference image of the solar vehicle is presented in Figure 3, which depicts all feasible aerodynamic and solar roof angle parameters from a manufacturing perspective. The vehicle, as depicted in Figure 4, measures 5.5 m in length, 1.6 m in width, and 1 m in height. Computational fluid dynamics analysis indicates a Cd of 0.0973, as shown in Figure 5, which illustrates the velocity pathlines of the vehicle. The vehicle is equipped with a 3.35 kWh battery pack and a 1.32 kWh solar panel.

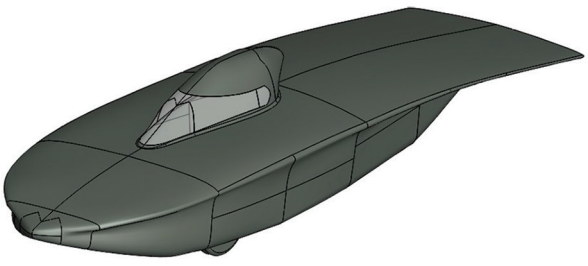

Figure 3. Isometric view of the solar vehicle

2.1. Solar energy input model

The WSC in Australia spans 3,000 km from Darwin to Adelaide, following the Stuart Highway, which offers clear visibility and predominantly dry weather conditions. Hottel's clear-day model[8] provides a simple method for calculating the transmittance of beam radiation. The only required inputs for this model are the elevation, day number, and zenith angle of the location, making it computationally efficient.[9] In addition, the deviation between the predicted and observed statistical results is minimal.[10] Relevant nomenclature is provided in Appendix. Table S1 lists altitude values necessary for estimating the coefficients in Equation I. Tables S2 and S3 provide the car's azimuth angles and the latitude values along the route, respectively – both of which are essential input variables for the model.

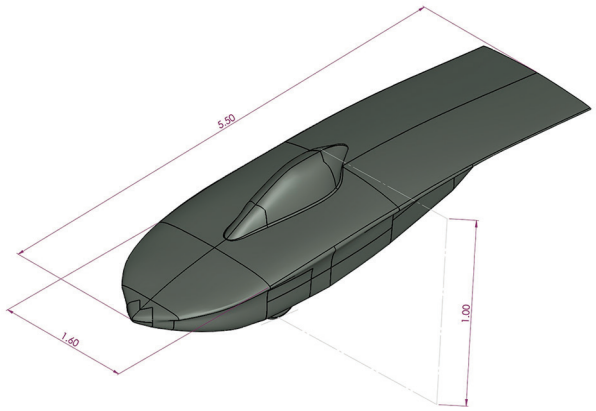

Figure 4. Dimensions (measurements in meters) of the solar vehicle

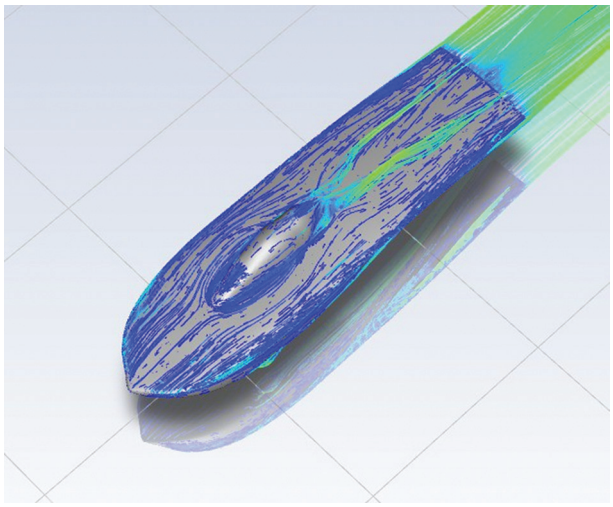

Figure 5. Simulated airflow over the solar vehicle

2.1.1. Empirical equations

Hoyt C. Hottel developed a set of equations to estimate the transmittance of direct solar radiation, considering elevation, longitude, the relative position of the Sun, and the solar collector angle under various climatic conditions. The transmittance is estimated using the model proposed by Hottel[8] in 1976:

$$\tau = a_0 + a_1 e^{k/\cos\theta} z \quad \text{(I)}$$

This model combines empirical relations from Hottel's clear-day model and Liu and Jordan's solar energy input model[11] to predict the total irradiance at a specific location. The following equations are used:

$$I_0 = I_s[1 + 0.034 \cos(360N/365.25)] \quad \text{(II)}$$

$$\delta = 23.45 \sin[360/365 + (284 + N)] \quad \text{(III)}$$

$$\omega = 15(t - 12) \quad \text{(IV)}$$

$$r_d = (1 + \cos\beta)/2 \quad \text{(V)}$$

$$\alpha = \sin^{-1}(\sin\delta \sin\phi + \cos\phi \cos\delta \cos\omega) \quad \text{(VI)}$$

$$\theta_z = 90 - \alpha \quad \text{(VII)}$$

$$I_b = I_0[A_0 + A_1 \exp(-k/\cos\theta_z)] \quad \text{(VIII)}$$

$$I_d = I_0 \cos\theta_z(0.2710 - 0.2939[A_0 + A_1 \exp(-k/\cos\theta_z)]) \quad \text{(IX)}$$

$$\text{solar}_{azimuth} = \tan^{-1}(2 \sin\omega/(\cos\omega \sin\phi - \tan\delta \cos\phi)) \quad \text{(X)}$$

$$\cos\theta_{ic} = \cos\theta_z \cos\beta + \sin\theta_z \sin\beta \cos\gamma - \text{solar}_{azimuth} \quad \text{(XI)}$$

$$r_b = \cos\theta_{ic}/\cos\theta_z \quad \text{(XII)}$$

$$I\text{total} = Ibrb + Idrd \quad \text{(XIII)}$$

2.2. Energy model

To conduct an energy audit for different scenarios, an energy model was employed to monitor all energy losses and gains during the race. Energy losses encompass aerodynamic drag, tire rolling resistance, road gradient, shadow effects, and motor winding loss. According to the regulations of the WSC 2025, teams are permitted a maximum of 11 MJ of stored energy and are only allowed to charge via the mounted solar panels, with specified solar areas for challenger-class competition vehicles. To account for energy gains, the model includes a fully charged 3.35 kWh battery pack and a solar collector with an area of 6 m^2, optimally angled for maximum exposure.

2.2.1. Empirical equations

The model incorporates empirical relationships for each type of loss and combines them to forecast total energy consumption over a 5-day period. Motor winding losses are derived from the manufacturer's technical data sheet. The efficiency of Maxeon's Ne3 solar cells is based on their current–voltage (I–V) curve, accounting for the efficiency reduction caused by lamination.[12] Figure 6 compares laminated and non-laminated configurations, illustrating how current and voltage vary under different irradiance conditions in Australia. In addition, the Elmar Solar MPPT, widely utilized by solar competition teams, operates within an optimized voltage input range and has a minimum threshold voltage of 20 V, below which the solar panel is not considered for power generation by the MPPT algorithm, as described in previous studies.[13] A Python code was developed to generate the energy profile across the full 5-day race duration. This enables predictive modeling of energy availability along the route, supporting more informed race strategy. The complete source code is provided in Supplementary Material 2 (Programmed python script to account for various losses and predict the energy profile and solar energy generation). In addition, Table S4 contains processed terrain and environmental data, including wind speed and angles recorded along the entire route during the WSC 2023. For accounting different losses, the following equations are used:

(i) Vehicle's parameter:

$$Drag_\tau = 0.5Cd\rho R_{tyre}(V_{sv}^2 + V_w^2 - 2V_{sv}V_w\cos\theta_w) \quad \text{(XIV)}$$

(ii) Motor modeling:

$$Wheel_\tau = R_{tyre}\, MgT_{crr} \cos\theta_s \quad \text{(XV)}$$

$$\tau = Drag_\tau + Wheel_\tau \quad \text{(XVI)}$$

(iii) Power loss equations:

$$T_\epsilon = 0.455(P_c + P_e) + T_a \quad \text{(XVII)}$$

$$B = 1.6716 - 0.0006(T_a - T_\epsilon) \quad \text{(XVIII)}$$

$$RMS_i = 0.561B\tau \quad \text{(XIX)}$$

$$R_\epsilon = 0.00022425T_\epsilon - 0.00820525 \quad \text{(XX)}$$

$$P_c = 3i^2R_\epsilon \quad \text{(XXI)}$$

$$P_e = 9.602 \times 10^{-6}(B / R_{tyre}^2) / R_\epsilon V_{sv}^2 \quad \text{(XXII)}$$

$$P_{out} = \tau V_{sv}/R_{tyre} \quad \text{(XXIII)}$$

$$P_\epsilon = V_{sv}^2 / (R_{tyre}^2 \times 170.4 \times 10^{-6})$$

$$P_{acc} = V_{sv}(M \times \text{acc} + Mg \sin\theta_s) \quad \text{(XXV)}$$

$$P_{net} = P_{out} + P_\epsilon + P_c + P_e + P_{acc} \quad \text{(XXVI)}$$

(iv) Energy audit equations:

$$Energy_{\text{consume}} = E(f(V_{sv}, \text{acc}, \theta_s, \theta_w, P_{\text{net}})) - \text{Solar}_{\text{input}} \quad \text{(XXVII)}$$

$$B.E._f = B.E._i - Energy_{\text{consume}} \quad \text{(XXVIII)}$$

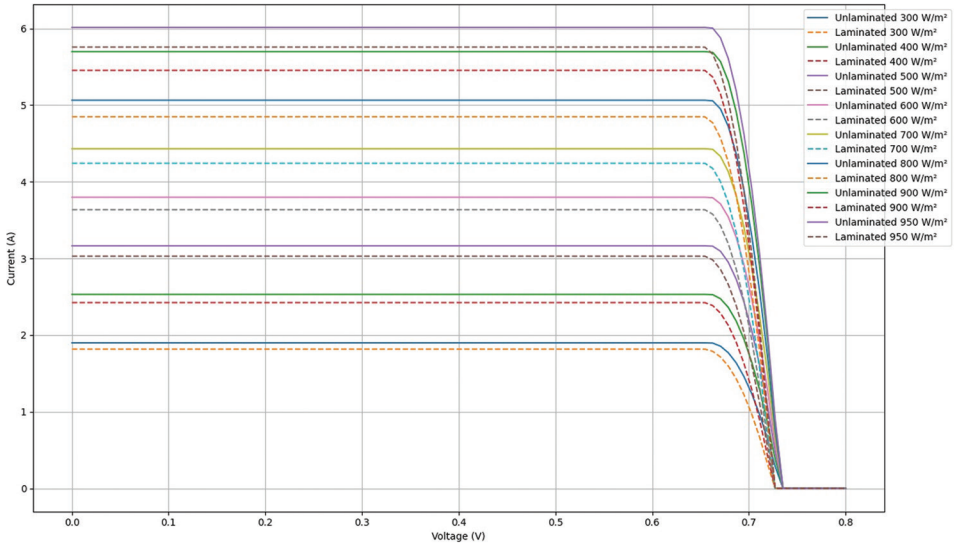

Figure 6. Current–voltage characteristics of SunPower Maxeon Ne3 solar cells under various irradiance levels expected in Australia. Graph created using data derived in Mateja *et al.*[12]

3. Methodology

The complex information flow used to identify shadow regions and their effects on energy generation is represented in Figure 7. The solar model was used to determine the optimal solar panel angle for enhancing energy input during the race. Among the calculated angles, only those that are practically feasible are considered as inputs to help achieve the targeted Cd value. In Figure 7, blue text indicates the model's input parameters. Vehicle position accounts for its latitude and longitude along the WSC route. The Sun's position is determined based on the vehicle's location and the time of day. Darwin's date and time are used as the standard reference – as mandated by the competition – to ensure consistency and avoid confusion during the race. Therefore, all calculations are performed based on Darwin time, not the local time of each location. Terrain information is input as road gradient, while the battery's state of charge (SOC) is monitored through the battery source. Motor losses are modeled using empirical relations provided by the supplier.

Yellow boxes in the diagram represent programmed prediction models that generate outputs such as energy consumption and solar energy (light green); the relevant equations are detailed later in this article. Dark green boxes represent viable solutions suggested to maximize solar energy output. Grey boxes denote iterative processes, such as identifying optimal solar angles to achieve the targeted Cd and recognizing shadow regions. These steps help reduce energy losses and enhance overall energy efficiency by informing measurable designs and control strategies for specific road segments.

Some limitations of the proposed methodology include the following:

- The final solar model averages irradiance across the entire route to optimize the roof for the full race, rather than analyzing conditions at every specific point
- The vehicle is assumed to face a particular angle, derived from the vehicle angle versus frequency graph (Figure 8)
- These data were generated using QGIS software (open-source).

Although the methodology and programmed models are optimized for WSC, they can be generalized by adjusting the input variables to suit other race routes or environmental conditions.

3.1. Vehicle's azimuth

The vehicle's position plays a crucial role in determining the amount of solar energy it receives. Factors such as latitude, altitude, and the relative position of the Sun and the vehicle must be considered. To accomplish this, we used QGIS, an open-source software, to mark points along the Stuart Highway. This allowed us to calculate the typical travel angle of the vehicle from Darwin to Adelaide relative to due north. This angle will aid us in determining the typical range of angles vehicles experience during the race and in assessing the shadow cast by the vehicle's canopy.

In Figure 8, the data show a concentrated spread of azimuth angles between 100° and 200°, indicating that most vehicle orientations fall within this range. Occasional outliers appear near 0° and 350°, while the most frequent orientations lie between 135° and 185°. By applying a frequency threshold of 9 and calculating the mean using the formula:

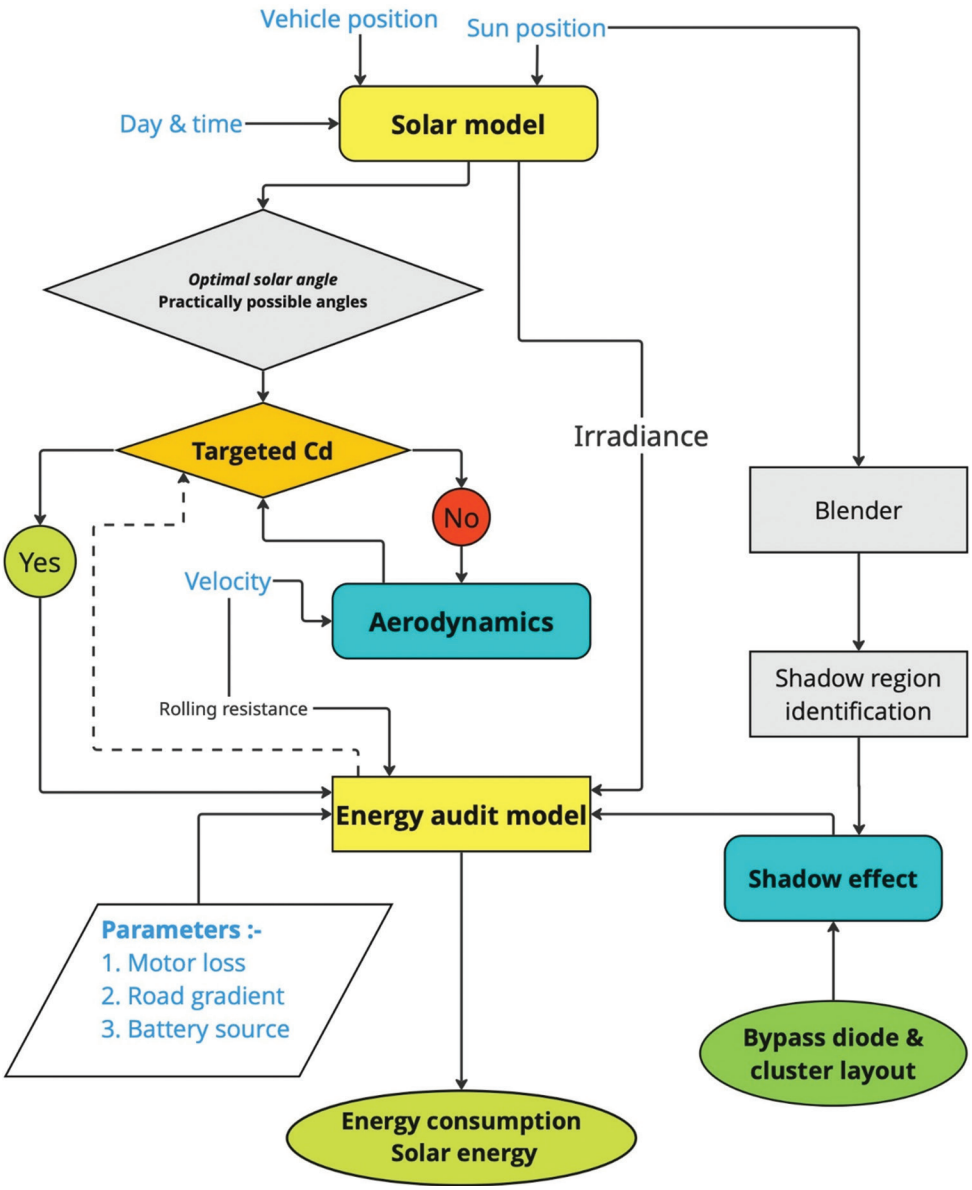

Figure 7. Information flow diagram for solar energy optimization in a competition vehicle. It illustrates the interactions between various models and input parameters to maximize solar energy capture.
Abbreviation: Cd: Drag coefficient.

$$\text{Mean} = \Sigma(f\,x)/\Sigma f \qquad \text{(XXIX)}$$

We obtain $Mean_{azimuth} = 159.92°$.

3.2. Shadow region

To accurately calculate the decrease in solar energy output during the race, it is essential to first identify the specific solar panel affected by shading. This can be achieved by leveraging the Sun's position data from the solar energy input model at different times and using it as input to Blender (open-source), a software platform that integrates the vehicle's computer-aided design model. By doing so, we can precisely pinpoint the shadowed region and determine its impact on solar energy collection. Identifying the affected solar panels is crucial for calculating the energy loss due to shadow throughout the race. Utilizing the Sun's position data as input to Blender enables precise visualization of shadow patterns on the vehicle's surface. Figure 9 highlights the solar panels most affected over prolonged periods during the race.

To measure the amount of energy lost due to shadows, a more methodical approach involves identifying the shadows within 20-min intervals. The panels affected by these

shadows are highlighted in Figures 10 and 11. This aids in simplifying the inputs for the solar and energy audit models, allowing for a more accurate accounting of shading effects.

3.3. Shadow effect: Limiting current

Partial shading of solar cell modules can severely restrict current flow through the entire module. Even minimal shading may cause individual cells to become reverse-biased, resulting in electrical power dissipation and a disproportionate decline in the overall module output. In addition, this phenomenon can trigger localized overheating, potentially causing thermal damage and compromising the module's structural integrity. In response to reduced current, unshaded cells adjust their operating points along their characteristic curves toward the open-circuit voltage. The resulting increase in voltage from these unshaded cells applies a reverse bias across the shaded cells, attempting to drive current through them. A promising solution to address this issue will be explored in subsequent sections.

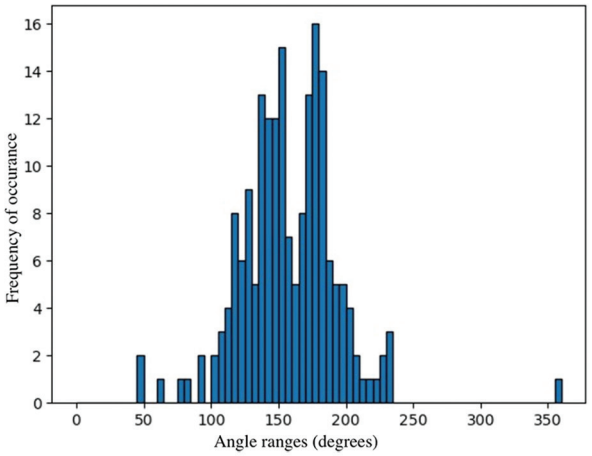

Figure 8. Histogram showing the distribution of vehicle angles with respect to frequency. The x-axis represents the angle ranges (in degrees), and the y-axis shows the frequency of occurrences for each range.

3.3.1. Bypass diodes

Bypass diodes are typically used to redirect current from unshaded solar cells, preventing it from flowing through shaded cells. This reduces the risk of thermal hotspots and minimizes power losses. Researchers have conducted detailed studies comparing the performance of solar arrays equipped with integral bypass diodes to those without such protection. Their findings indicate that arrays with bypass diodes consistently achieve higher maximum power point output under various shading scenarios.[14]

To enhance energy output efficiency, Hasyim *et al.*[14] recommends integrating bypass diodes into each cell of the solar array. However, this approach may not be cost-effective in all cases. An estimation is currently being conducted to determine the number of bypass diodes required for a group of n solar cells, with a safety margin

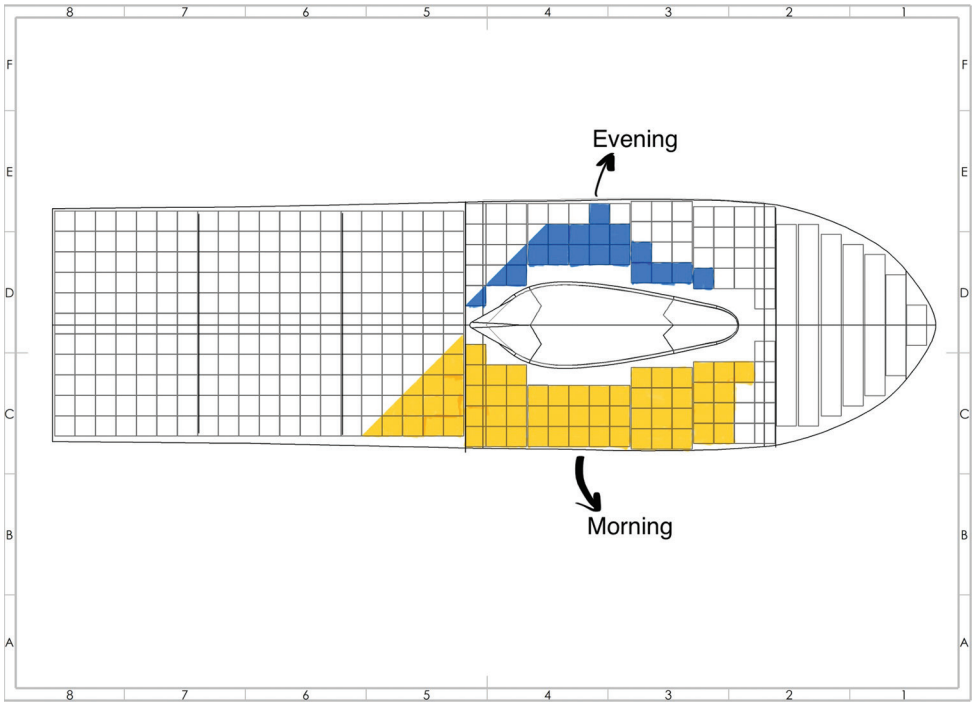

Figure 9. Illustration of solar panels affected by shadows cast by the driver's canopy. Panels shaded in yellow are affected in the morning (8:30 – 10:00 AM), while those in blue are likely to be affected in the evening (4:00 – 5:00 PM).

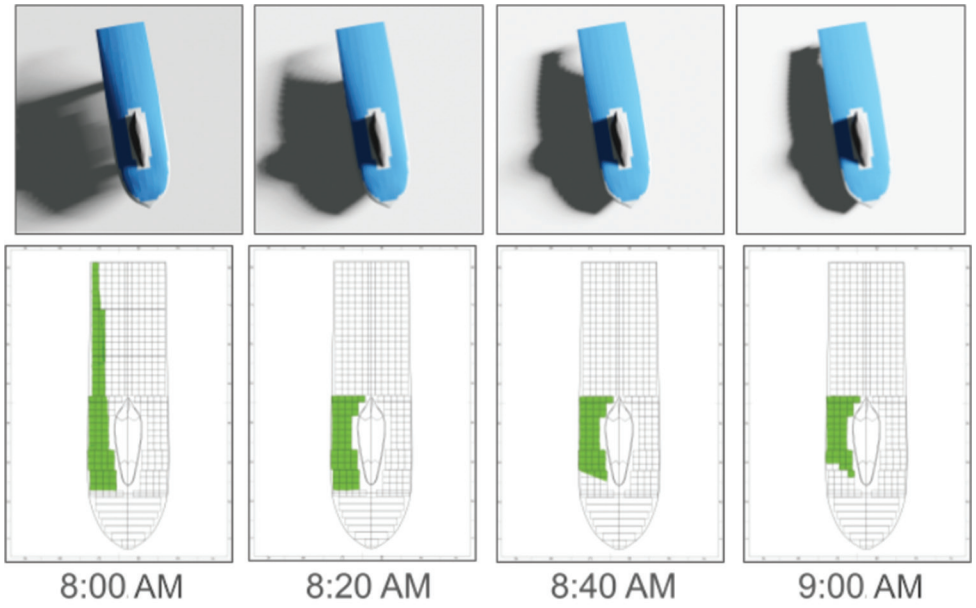

Figure 10. Blender visualization of shadow affected area from 8:00 AM to 9:00 AM on top with corresponding solar panels highlighted below to extract affected cells

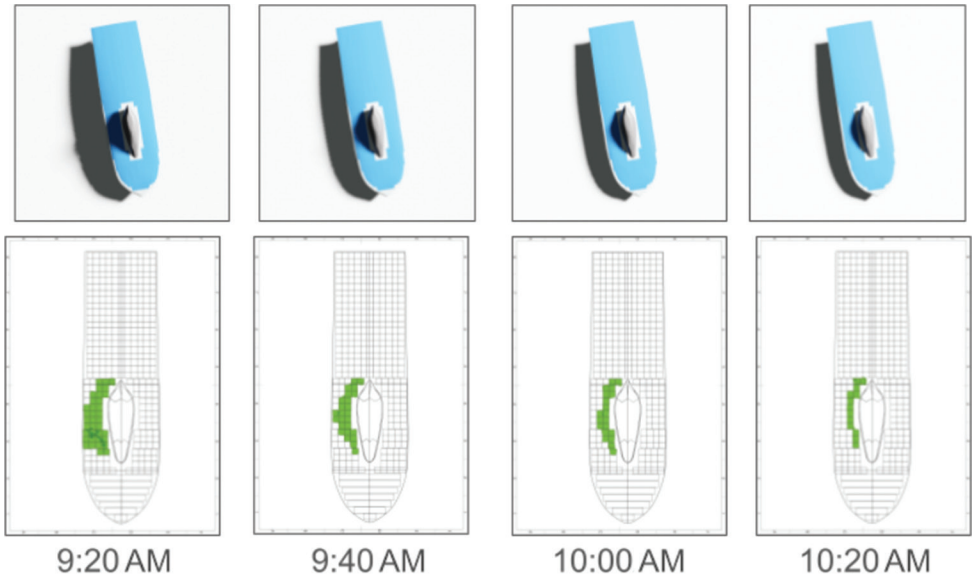

Figure 11. Blender visualization of shadow affected area from 9:20 AM to 10:20 AM on top with corresponding solar panels highlighted below to extract affected cells

set at 80% of the breakdown voltage. According to Silvestre *et al.*,[15] at least one diode should be installed for every 16 cells, based on factors such as shaded cell voltage, diode voltage, open-circuit voltage, and breakdown voltage.

Temperature effects must also be considered when determining the appropriate number of bypass diodes. Under adverse working conditions, the temperature of the shaded cell may rise, potentially causing irreversible damage to the cell or its encapsulation.

To estimate the limiting current of the solar panels, data extrapolation under low-irradiance conditions is required. Figure 12 follows a trend similar to Figure 6, particularly in the laminated case.

4. Optimization and solution

To maximize solar energy input during the race, it is important to set the solar angle to the most optimal angle while fulfilling all system constraints. In addition, different

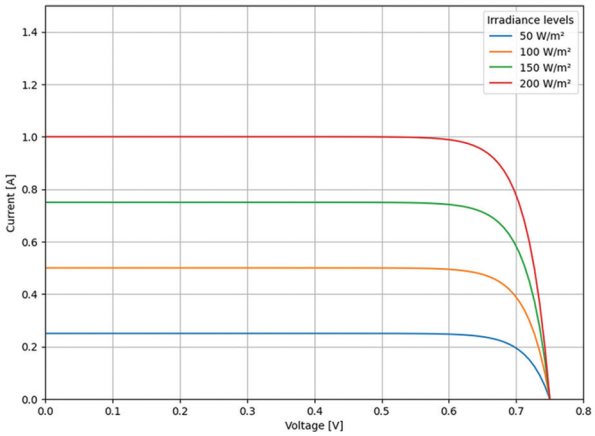

Figure 12. Extrapolated current–voltage characteristics for SunPower Maxeon Ne3 cells at various irradiance levels

clustering arrangements can be explored, as they respond differently under identical shadow conditions. Selecting the configuration that best suits operational needs is important, and these data are particularly valuable for making strategic decisions – such as determining when to accelerate or predicting the optimal times to minimize or maximize energy usage during the race.

4.1. Clustering arrangements

Various cluster arrangements are considered, as the minimum required input voltage from the array is 20 V, as mentioned in Section 2.2.1. These arrangements lead to different energy outputs for solar cells under similar shading conditions. Another important constraint is the maximum number of cells that can be connected to a single MPPT unit, which is typically limited to 77 – 78 cells. For the entire 6 m^2 solar array, approximately 384 Ne3 solar cells are used, each measuring 0.15 m × 0.15 m. These are organized into six clusters, with each cluster connected to its own MPPT. Figures 13-16 illustrate the clustering arrangement.

4.2. Optimal roof angle

As mentioned earlier, the regulations for WSC2025 have been updated to allow a solar panel area of up to 6 m^2. There is now a stronger emphasis on designing vehicles that efficiently harness renewable energy, aligning with new initiatives for sustainable mobility. The angle of the solar panels is crucial for optimizing energy capture. In stationary solar grids, various sensors are typically used to track the Sun's position and adjust panel angle accordingly to ensure consistent energy generation throughout the day. However, solar vehicles do not incorporate such tracking mechanisms due to the weight constraints and practical limitations during motion. Integrating servo motors for sun tracking would require additional energy, reducing the vehicle's overall efficiency.

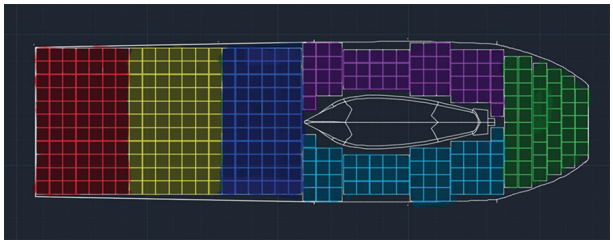

Figure 13. Cluster 1 configuration

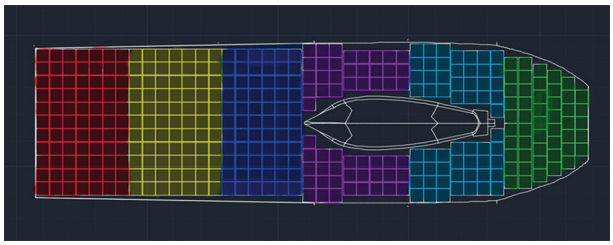

Figure 14. Cluster 2 configuration

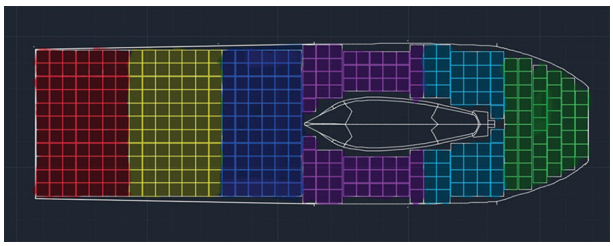

Figure 15. Cluster 3 configuration

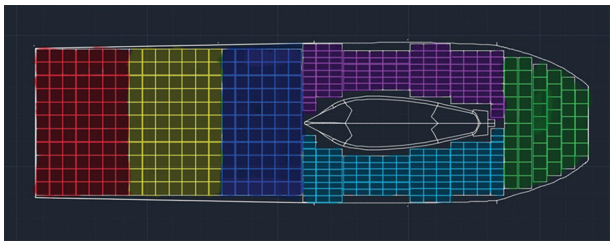

Figure 16. Half-cut cells cluster: Each cell is connected in parallel to double the voltage and is placed in regions most affected by shadow

5. Results and discussion

5.1. Application of the solar model for performance enhancement

Integrating the various factors that influence solar energy production is essential for accurately predicting energy consumption behavior during the race. This predictive capability is critical for both strategic development and vehicle design. The results from the solar energy input model, as depicted in Figures 17 and 18, illustrate how

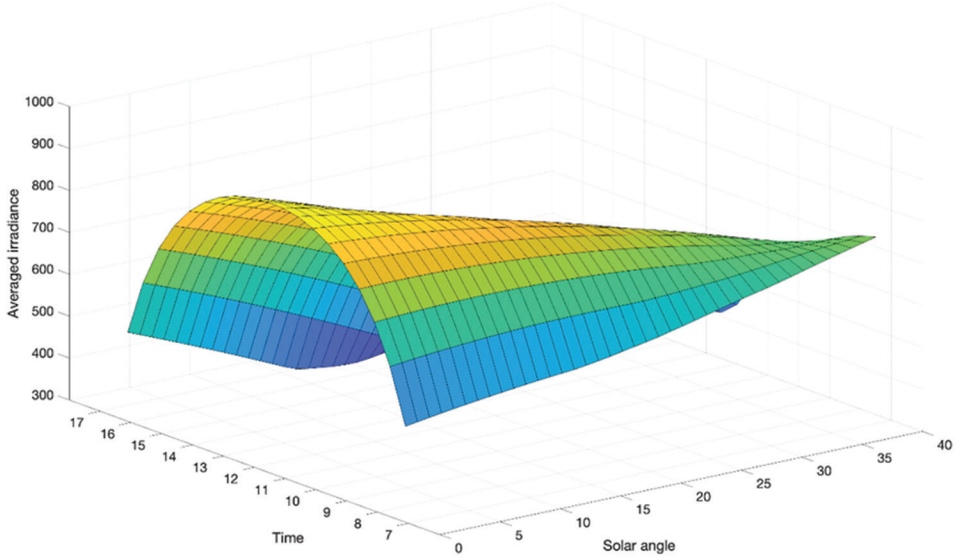

Figure 17. 3D surface plot showing the averaged solar irradiance (in W/m²) received by the solar panel throughout the day (7:00 AM – 5:00 PM) at varying panel angles. The plot highlights the irradiance pattern as a function of time and angle, helping identify optimal angles for maximum energy capture.

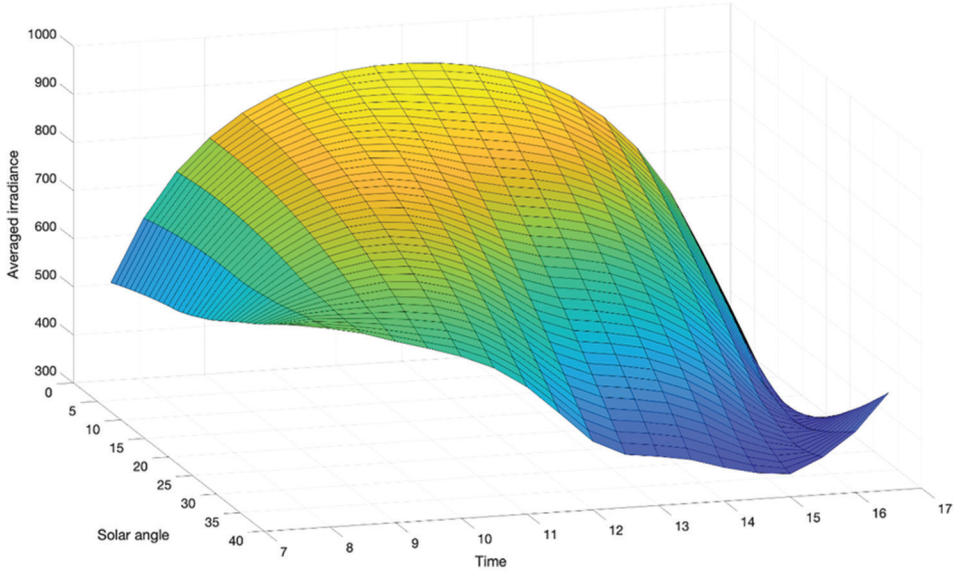

Figure 18. Inverted perspective of the averaged solar irradiance (in W/m²) across the day and varying solar angles. This alternative view enhances the visualization of irradiance distribution and facilitates the comparison of different time–angle configurations.

varying solar array angles affect solar irradiance on the surface over a designated time frame. To optimize energy input, it is imperative to maintain the solar panels at these optimal angles. This energy input informs the aerodynamic team in shaping the vehicle's exterior to ensure that optimal angles are maintained across different sections of the vehicle.

The vehicle is divided into three primary sections: the front section (extending up to the canopy), the midsection (adjacent to the canopy), and the tail section (located behind the canopy). The findings indicate that during the early hours of the race (8:00 – 9:00 AM) when the Sun is closer to the horizon, a sideways curvature in the mid and tail sections of the roof enhances solar irradiance capture. Meanwhile, the front section is typically angled between 15° and 20° for aerodynamic optimization. As the day progresses and the Sun rises higher, it becomes more beneficial to have a flatter solar roof (0°), as irradiance

is higher and more energy can be stored. Similarly, the tail section of the vehicle, which often features a slight curvature of 0 – 5°, contributes to both drag reduction and increased irradiance capture.

A similar trend of flatter angles is observed in the late afternoon (4:00 – 5:00 PM). This is because the Sun is still relatively high, unlike the sharp angle seen during early morning hours, and there is still ample time before sunset.

Another important insight illustrated by Figures 17 and 18 is the significance of control stops, as required by race rules. These designated stops allow vehicles to charge using solar energy. The irradiance curves can be used to adjust the roof angles based on the time of the day, maximizing solar input during stationary charging periods. Figure 19, generated using SunEarthtools.com, illustrates the Sun's elevation and azimuth angles for Alice Springs. This graph supports the irradiance behavior shown in Figures 17 and 18 and provides further insights into optimizing solar panel orientation based on the Sun's position, thereby enhancing overall solar energy capture.

5.2. Application of the energy audit model for performance enhancement

The output from the energy audit model, illustrated in Figures 20 and 21, elucidates the impact of shading on the energy consumption profile. The ideal I-V cluster reflects a scenario free from shadow interference on the solar panels, with cell efficiencies ranging from 23% to 24%. Clusters 1, 2, and 3 are represented in Figures 13-15, respectively. The half-cut cell profile (Figure 16) employs half-cut Ne3 cells in areas more susceptible to prolonged shadowing. The Cluster 1-No Diode profile replicates the layout of Cluster 1 but excludes bypass diodes from all solar panels. In contrast, the Const-Efficiency cluster retains the Cluster 1 configuration but assumes an efficiency of approximately 19% for the Ne3 cells under shadow conditions.

The power output versus time graph presented in Figure 20 provides a comprehensive understanding of the energy harvested from the solar panels across the aforementioned cluster arrangements throughout the day. This study aims to investigate the impact of shadow regions on solar energy input in solar vehicles, particularly those participating in the WSC, and to integrate this understanding into the energy prediction model for improved race strategy planning.

By examining the battery level versus time graph in Figure 21, we can observe distinct energy consumption patterns. In the ideal model (with no shadow effect and maximum Ne3 cell efficiency), energy availability is significantly higher compared to the shadowed cluster configurations. This overestimation in ideal conditions may be misleading for real-world race scenarios.

From Day 1 to 9:00 AM on Day 3, increased energy usage is observed due to the vehicle traversing uphill gradients, requiring more energy to overcome elevation gain. Afterward, a descent – confirmed by elevation data – results in decreased energy consumption, which is reflected in the energy model outputs.

The slope of the energy profile depicts different energy flow scenarios:

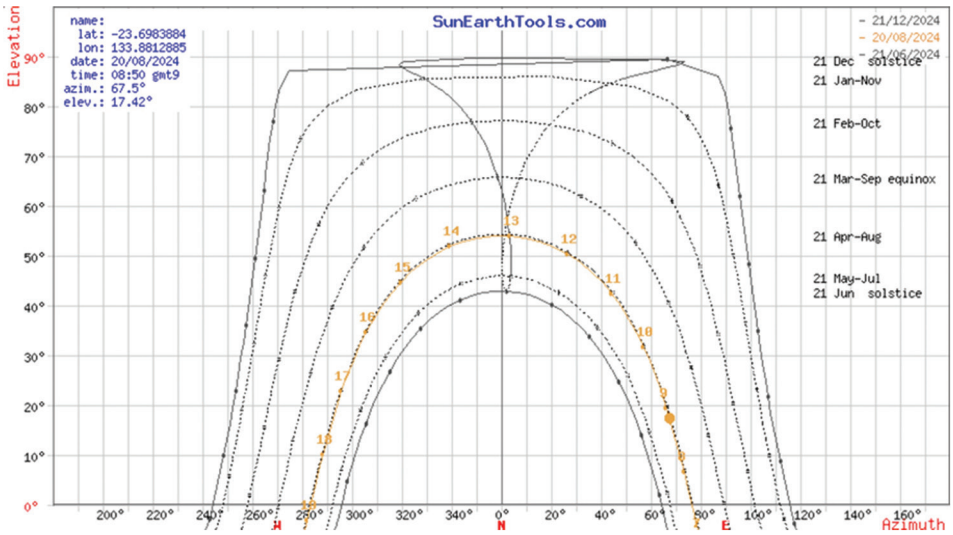

Figure 19. Sun path diagram for Alice Springs (latitude: −23.6984°, longitude: 133.8813°). The highlighted path corresponds to August 20, 2024, and shows the Sun's elevation and azimuth angles.
Source: SunEarthtools.com.

- Positive slope: surplus energy is produced and stored in the battery (charging)
- Negative slope: energy demand exceeds solar input (discharging)
- Zero slope: energy input matches consumption (neutral energy state).

Different clusters follow the same general trend but vary in energy production. A clearer understanding can be obtained from Figure 20, which shows that all cluster arrangements behave differently between 8:00 AM and 10:00 AM, even under identical shading conditions. Among them, the half-cut cell cluster outperforms the others. This disparity arises from the minimum voltage requirement of the MPPT, as discussed earlier in Section 2.2.1.

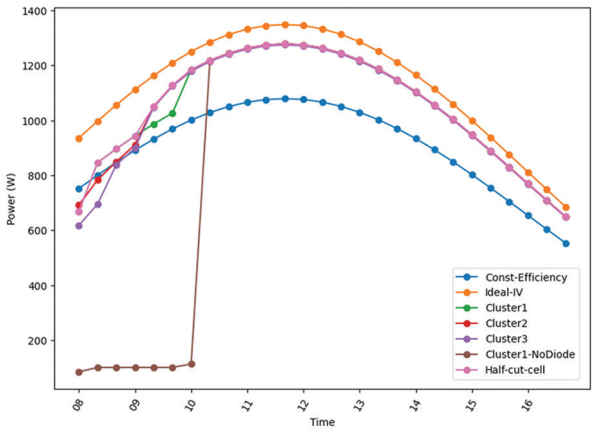

Figure 20. Solar energy output is managed by the maximum power point tracking system over a single race day, for various cluster arrangements. Each curve corresponds to a specific cluster setup, showing how power output varies throughout the day as solar irradiance changes. This analysis is critical for understanding the performance of each configuration in harvesting solar energy.

The half-cut cell design offers greater reliability by delivering double the voltage and half the current when connected in series. As a result, resistive losses are significantly reduced compared to full-cut cells. In addition, half-cut solar cells are approximately 3% more efficient under shading conditions and generate 223.35 W more electricity over the entire race.

Clusters 1, 2, and 3 each yield different power outputs depending on their arrangement and are similarly constrained by the MPPT's minimum voltage input. The Const-Efficiency curve represents solar panels operating at 19% efficiency with shadow effects. All clusters – except the ideal and Const-Efficiency configurations – exhibit a drop in energy output after 10:00 AM, even when the shadow effect is no longer an important factor. This is attributed to efficiency losses from panel lamination and inter-cell tabbing losses, as discussed in Figure 6. From the graph, we observe that the Cluster 1-No Diode configuration performs the worst among all. As discussed in Section 3.3, this is due to limiting current effects, which prevent effective energy flow when shading occurs. Consequently, this arrangement fails to complete the race within the required time, as shown in Figure 21. Even the Const-

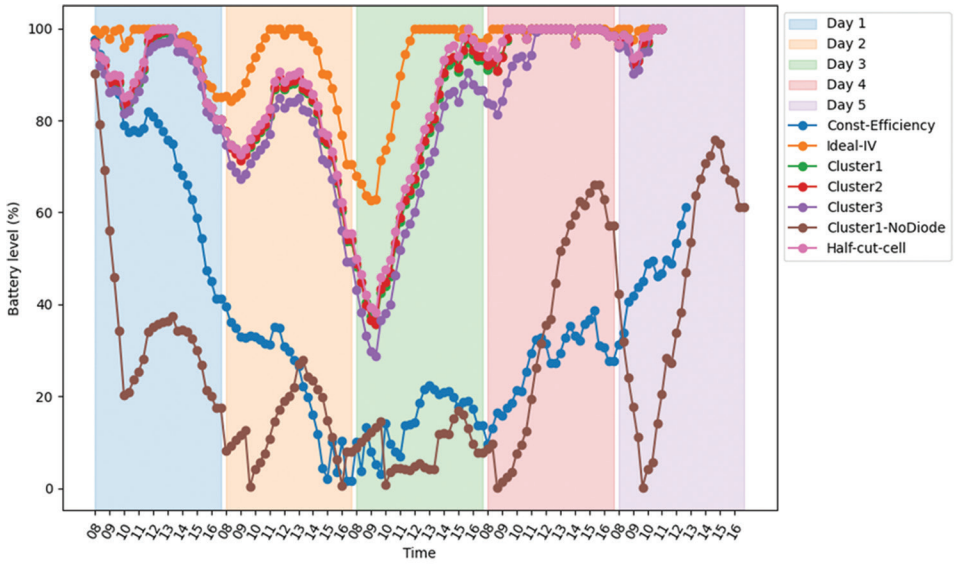

Figure 21. Battery level over 5 days, with each curve representing a different cluster arrangement (as described in Section 4.1). The slope of each curve represents energy flow: positive (charging), negative (discharging), and flat (steady state). Background shading highlights each day to enable visual comparison across configurations.

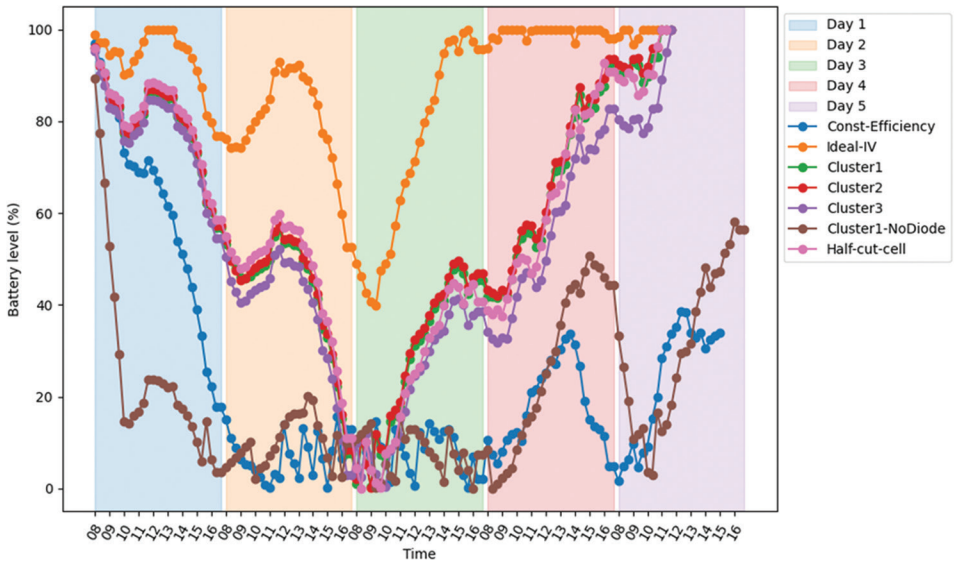

Figure 22. Sensitivity analysis showing the impact of a 10% increase in aerodynamic drag on vehicle performance across different cluster configurations

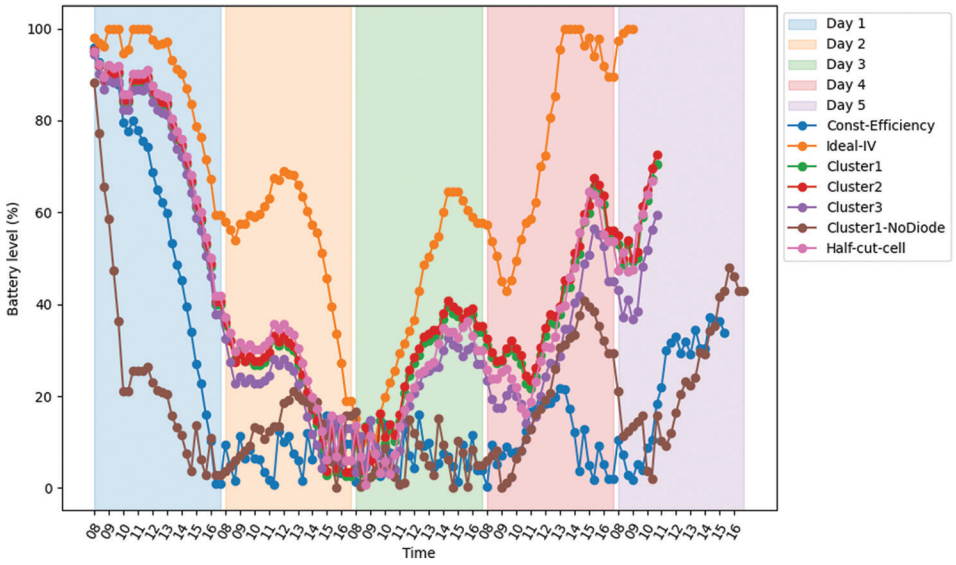

Figure 23. Sensitivity analysis showing the impact of vehicle velocity to 85 km/h on energy performance across various cluster configurations

Efficiency configuration requires more time to complete the race compared to other cluster arrangements.

These findings highlight the importance of considering shadow effects within the race strategy and energy prediction models. The results also underscore the significance of using bypass diodes. As discussed in Section 3.3.1, some approaches recommend integrating bypass diodes into every solar cell, while others suggest placing them selectively between groups of cells to avoid permanent damage.

To maintain performance while ensuring cost-effectiveness, a practical solution involves:

- Identifying shadow-prone regions of the vehicle,
- Using fewer bypass diodes in unshaded areas
- Implementing integrated bypass diodes only in areas exposed to shadow.

The use of half-cut cells in the shadow region can also improve energy capture. These cells are especially suitable for compact areas like the midsection of the vehicle and are widely adopted by many solar vehicle teams due to their

layout flexibility and enhanced performance under partial shading.

The presented results assume a constant vehicle speed, with no acceleration or deceleration throughout the race. Under these conditions, it was observed that when panel efficiency drops to 19%, the total available energy approaches zero. This situation may lead to disqualification, as the vehicle would no longer be capable of operating safely. Operating the battery at such low SOC levels is also considered risky.

A possible solution is to reduce the vehicle speed to the minimum permissible limits of 65 – 70 km/h. However, this also increases the risk of not completing the race on time. While this model provides a general outline of the shadow effect, a more sophisticated energy model that accounts for variable velocity and regenerative braking should be considered for further micro-optimization and more effective strategic planning.

Another dimension to consider when optimizing solar electric vehicles is the social, functional, environmental, and cultural framework, and its implications during product development, as discussed in past literature.[16] While the current focus is on developing solar electric vehicles exclusively for the WSC, this approach does not fully address the social and functional aspects of vehicle design.

For instance, the vehicle may only be driven by individuals weighing <80 kg to minimize weight, which introduces a social equity issue by excluding certain participants. In addition, the high cost of producing such a vehicle raises concerns about economic accessibility, representing a form of economic injustice.

Although these considerations may be justifiable in a competition setting – where the primary focus is on perceptual outreach to promote sustainable transportation in the future – they become more significant when designing energy-efficient solar electric vehicles for commercial deployment or broader, more inclusive competitions.

These types of risk assessment strategies may be explored as part of future work.

5.3. Sensitivity analysis

As the models rely on empirical equations and computational fluid dynamics results to derive input values, errors in these inputs can lead to inaccurate predictions. Therefore, it is recommended to use real-time inputs such as irradiance and battery SOC during the competition. In addition, the final Cd value of the vehicle should be determined through aerodynamic testing and used in the energy prediction model.

Among all input parameters, the Cd value is the most sensitive. Even a 1% increment in Cd results in a corresponding increase in aerodynamic force, which can significantly impact the overall energy prediction. This sensitivity is illustrated in Figure 22, where the battery drains more rapidly under increased drag, causing some cluster profiles to fall below the critical 20% battery level, potentially leading to disqualification. Hence, maintaining the vehicle's Cd within permissible limits is crucial. However, this parameter is particularly challenging to control, as it is heavily influenced by the vehicle's surface finish – a feature that is difficult to manage consistently during manufacturing. Therefore, accurate Cd testing for the final vehicle is essential to inform race strategies. On the other hand, parameters such as electrical losses are well-accounted for and provided by the supplier based on experimental validation. These parameters are more manageable. Other parameters, such as velocity, are also sensitive but can be integrated into a data-driven prediction model to determine an optimal velocity that minimizes energy consumption. The sensitivity of vehicle velocity is demonstrated in Figure 23, where driving at high speed during the uphill segments (particularly in the early stage of the race) poses a substantial risk. It is therefore advisable to increase velocity during downhill sections. In this analysis, all cluster profiles dropped below the 20% battery level, indicating a high risk of elimination from the competition. Hence, a predictive velocity model is urgently needed.

6. Conclusion

This study investigated the influence of shadow regions on solar energy input and explored strategies to minimize their impact on solar vehicles participating in WSC. Our findings revealed that optimizing the roof angle – while considering practical and aerodynamic constraints – is crucial to enhancing solar energy input during the race. By accounting for the vehicle's position and the Sun's azimuth, half-cut solar cells were identified as the most efficient solution. These cells not only improve total power input during the race, accounting for the shadow but also provide flexibility in their roof placement.

This cluster arrangement is particularly effective when shadow regions persist for extended periods, as it enables the vehicle to maintain operation above the minimum voltage input threshold. To achieve outcomes that closely align with the energy audit model, effective planning of bypass diodes is essential to ensure both economic and efficient performance. Identifying the shadow-affected regions of the solar panels, as illustrated in Figure 9, aids in selecting panels where bypass diodes should be integrated into each solar cell.

Furthermore, the solar energy model and energy audit model employed in this study can be adapted for tropical countries with arid to semi-arid climates and minimal cloud cover, such as India in the Northern Hemisphere and South Africa in the Southern Hemisphere. This methodology also holds promise for competitions such as the Sasol Solar Challenge, thereby contributing to the advancement of solar vehicle technology.

While this research primarily focused on mitigating the shadow effect, future studies should aim to model more complex scenarios involving dynamic race conditions and predict optimal driving velocities for micro-optimization and improved strategic planning. During the competition – where conserving energy is a key priority – solar vehicles typically maintain speeds of 75 – 80 km/h. Although the current energy model accurately predicts energy consumption during the race, a more dynamic model that considers acceleration and deceleration across varying terrain would enable real-time energy-saving decisions. While this would impact energy prediction accuracy, it would not alter the shadow regions identified or their associated losses.

The current model accounts for a range of significant system-level losses and closely reflects real-world performance. Therefore, it can serve as a valuable baseline for vehicle design and strategic planning. Advancements in solar energy optimization and vehicle design are crucial for propelling the future of sustainable automobiles. This includes selecting appropriate composite materials, such as carbon fiber, to reduce vehicle weight. Further research is needed to develop more efficient PV technologies, such as perovskite tandem cells. In addition, vehicle design should aim to minimize drag and optimize performance in response to external factors, such as irradiance and shadow regions.

The combined efficiency of these systems contributes to the commercialization of solar electric vehicles. Furthermore, optimizing solar energy, particularly with respect to roof angle and shadow regions, not only enhances competitive performance but also lays the foundation for developing commercial solar vehicles with extended endurance. These advancements in sustainable automotive technology pave the way for innovations such as onboard solar charging, which could significantly reduce charging times and extend driving range, making this a key area for future research.

Acknowledgments

None.

Funding

None.

Conflict of interest

K. S. Reddy is an Editorial Board Member of this journal but was not in any way involved in the editorial and peer-review process conducted for this paper, directly or indirectly. Separately, other authors declared that they have no known competing financial interests or personal relationships that could have influenced the work reported in this paper.

Author contributions

Conceptualization: Pradyum Kaneria
Data curation: Pradyum Kaneria
Methodology: Pradyum Kaneria
Project administration: K. S. Reddy
Software: Pradyum Kaneria
Supervision: K. S. Reddy
Visualization: Pradyum Kaneria
Writing-original draft: Pradyum Kaneria
Writing-review & editing: K. S. Reddy

Ethics approval and consent to participate

Not applicable.

Consent for publication

Not applicable.

Availability of data

On request, the code file and supplementary material will be provided.

References

1. Veerapen S, Wen H. Shadowing Effect on the Power Output of a Photovoltaic Panel. In: *2016 IEEE 8th International Power Electronics and Motion Control Conference (IPEMC-ECCE Asia)*. United States: IEEE; 2016. p. 3508-3513.

   doi: 10.1109/IPEMC.2016.7512858

2. Du J, Xu R, Chen X, Li Y, Wu J. A Novel Solar Panel Optimizer with Self-Compensation for Partial Shadow Condition. In: *2013 Twenty-Eighth Annual IEEE Applied Power Electronics Conference and Exposition (APEC)*. 2013. p. 92-96.

   doi: 10.1109/APEC.2013.6520190

3. Kazem HA, Chaichan MT, Alwaeli AH, Mani K. *Effect of Shadows on the Performance of Solar Photovoltaic*. Germany: Springer eBooks; 2016. p. 379-385.

   doi: 10.1007/978-3-319-30746-6-27

4. Ku J, Kim SM, Park HD. Energy-saving path planning navigation for solar-powered vehicles considering shadows. *Renew Energy*. 2024;236:121424.

   doi: 10.1016/j.renene.2024.121424

5. Brito MC, Santos T, Moura F, Pera D, Rocha J. Urban solar potential for vehicle integrated photovoltaics. *Transp Res Part D Transp Environ.* 2021;94:102810.

doi: 10.1016/j.trd.2021.102810

6. Birnie DP 3rd. Analysis of energy capture by vehicle solar roofs in conjunction with workplace plug-in charging. *Solar Energy*. 2016;125:219-226.

doi: 10.1016/j.solener.2015.12.014

7. ElMenshawy M, ElMenshawy M, Massoud A, Gastli A. Solar car efficient power converters' design. In: *2016 IEEE Symposium on Computer Applications and Industrial Electronics (ISCAIE)*. United States: IEEE; 2016. p. 177-182.

doi: 10.1109/ISCAIE.2016.7575059

8. Hottel HC. A simple model for estimating the transmittance of direct solar radiation through clear atmospheres. *Solar Energy*. 1976;18(2):129-134.

doi: 10.1016/0038-092x(76)90045-1

9. Islahi A, Shakil S, Hamed M. Hottel's clear day model for a typical arid city-Jeddah. *Int J Eng Sci Invent*. 2015;4:32-37.

10. Kassem Kh O. Estimation of clear-sky global solar radiation using hottel's model and Liu and Jordan's model for Qena/ Egypt. *Res Environ*. 2021;11(1):9-17.

doi: 10.5923.j.re.20211101.02

11. Liu BYH, Jordan RC. The interrelationship and characteristic distribution of direct, diffuse and total solar radiation. *Solar Energy*. 1960;4(3):1-19.

doi: 10.1016/0038-092X(60)90062-1

12. Mateja K, Skarka W, Drygała A. Efficiency decreases in a laminated solar cell developed for a UAV. *Materials*. 2022;15(24):8774.

doi: 10.3390/ma15248774

13. Elmar. *Elmar Solar Race MPPT Datasheet*; 2021. Available from: https://docs.prohelion.com/MPPTs/pdfs/Elmar%20Solar%20MPPT%20Race%202021.pdf

14. Hasyim ES, Wenham SR, Green MA. Shadow tolerance of modules incorporating integral bypass diode solar cells. *Solar Cells*. 1986;19(2):109-122.

doi: 10.1016/0379-6787(86)90036-0

15. Silvestre S, Boronat A, Chouder A. Study of bypass diodes configuration on PV modules. *Appl Energy*. 2009;86(9):1632-1640.

doi: 10.1016/j.apenergy.2009.01.020

16. Spreafico C, Sutrisno A. Artificial intelligence assisted social failure mode and effect analysis (FMEA) for sustainable product design. *Sustainability*. 2023;15(11):8678.

doi: 10.3390/su15118678

Appendix

Nomenclature				
Constants				
g Acceleration due to gravity	9.81 m/s^2	A_1	Hottel's clear-day constant	—
ρ Air density	1.192 kg/m^3	k	Hottel's clear-day constant	—
Cd Coefficient of drag of vehicle	0.0973	M	Mass of vehicle[a]	267 kg
A_0 Hottel's clear-day constant	—	I_s	Solar constant	1,367 W/m^2
Symbols				
θ Angle	Degrees	P	Power loss	Joule/s
$B.E._i$ Battery energy	10.998 MJ	r	Radiation	W/m^2
δ Dip angle	Degrees	R_{tyre}	Radius of tyre	0.2785 m
α Elevation angle	Degrees	T_{crr}	Rolling resistance	0.0045
ω Hour angle	Degrees	RMS_i	RMS phase current	Ampere
I Irradiance	W/m^2	β	Solar collector angle	Degrees
ϕ Latitude	—	T	Temperature	°C
B Magnetic remanence	Tesla	t	Time in 24-hour format	—
N Number of day	—	V	Velocity	m/s
Subscripts				
acc Acceleration		i	Initial	
a Ambient	22°C	s	Road gradient	
b Beam		sv	Solar vehicle	22.2 m/s
c Copper (ohmic)		out	Vehicle kinetic loss	
d Diffused		w	Wind	
e Eddy current		ϵ	Winding	
f Final		z	Zenith	
ic Incident angle				

Note: [a]including an 80 kg driver.